Zeolites

DOI: 10.1002/ange.200803103

Nanoscale Reactor Engineering: Hydrothermal Synthesis of Uniform Zeolite Particles in Massively Parallel Reaction Chambers**

*Won Cheol Yoo, Sandeep Kumar, Zhiyong Wang, Nicholas S. Ergang, Wei Fan, Georgios N. Karanikolos, Alon V. McCormick, R. Lee Penn, Michael Tsapatsis, and Andreas Stein**

Nanocasting is a powerful technique for molding materials with nanostructures that are dictated by a porous preform, such as a micro-, meso-, or macroporous solid.[1] The pores are filled with precursors for the desired product. After processing and removal of the preform, replica structures are obtained. Micromolding techniques in inverse opals or "lost wax templating" methods have been used to generate replica opal structures or monodisperse spherical particles that resemble the shape of pores in the inverse opal.[2] The concept of synthesizing nanoparticles in confined environments[3] has also been applied to block copolymer micelles, miniemulsions, polymer microgels, and similar "soft" molds.[4] Among the range of materials prepared by nanocasting, nanosized[5] and uniformly shaped[6] zeolite particles have been synthesized in the confinement of mesoporous carbon, which forms a matrix that is resistant to hydrothermal (HT) processing conditions and is easily removed by combustion.[7] In those studies, the role of the porous carbon matrix was mainly to physically confine the product within the pore space in order to impose the shapes and dimensions of the pores onto the product structure, irrespective of the gel composition.[5] Herein we demonstrate that three-dimensionally ordered macroporous (3DOM) carbon matrixes can act as massively parallel reaction chambers for high-yield HT syntheses of zeolite particles with uniform sizes (in this case the molecular sieve TPA-silicalite-1); the product morphology is controlled not only by the shape of the macropores but also by several parameters that can be designed into the nanoreactor structure or adjusted during HT processing. These include the charge of polyelectrolytes deposited on the surface of the porous host, the precursor concentration, the number of infiltration steps, the proximity of a pore to the monolith exterior, and the dimensions of windows that connect adjacent pores and define transport properties. Depending on these parameters, the products can be uniform solid spheres; geode-like, hollow zeolite spheres; or colloidal crystal arrays of such spheres. The sphere surface may be smooth or corrugated. Under specific conditions, needle-shaped zeolite particles can also be manufactured. Such particles with controllable shapes and defined dimensions are of great interest for preparations of hierarchically structured zeolite catalysts. This nanoreactor engineering approach promises improved control over the morphology of materials prepared by confined syntheses, and the design principles should also be applicable to HT syntheses of other materials.

3DOM carbon[8,9] is a suitable reactor for HT processing of small particles because of its unique architecture, its chemical stability under HT synthesis conditions, and because it can be prepared in monolithic form, which facilitates removal of any excess deposits on external surfaces. 3DOM C was synthesized by an established colloidal crystal templating method using a resorcinol formaldehyde precursor.[9] After template removal, the structure consists of a carbon framework that surrounds uniform spherical voids (Figure 1). Importantly, all macropores (or reaction vessels) are inter-

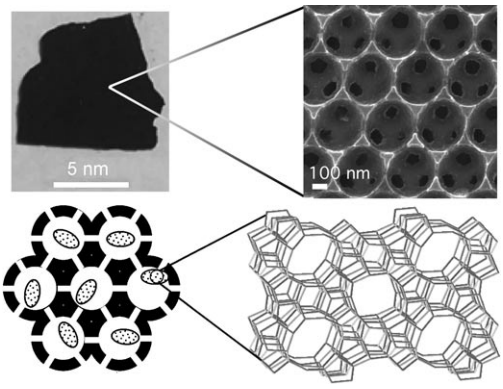

Figure 1. The nanoreactor concept. A 3DOM C monolith (photograph top left) contains massively parallel macropores that are interconnected through smaller windows (black circles in the SEM image, top right). Each macropore may be considered as a separate reaction vessel that permits nutrient exchange but limits exchange of silicalite crystals between adjacent pores (bottom).

[*] W. C. Yoo, Z. Wang, Prof. R. L. Penn, Prof. A. Stein
Department of Chemistry
University of Minnesota, Minneapolis, MN 55455 (USA)
Fax: (+1) 612-626-7541
E-mail: a-stein@umn.edu
Homepage: http://www.chem.umn.edu/groups/stein
S. Kumar, Dr. N. S. Ergang, Dr. W. Fan, Dr. G. N. Karanikolos, Prof. A. V. McCormick, Prof. M. Tsapatsis
Department of Chemical Engineering & Materials Science
University of Minnesota, Minneapolis, MN 55455 (USA)

[**] Funding was provided by the NSF (mainly by CMMI-0707610 and in parts by DMR-0704312, DMR-0212302 and CBET-0522518) and the Petroleum Research Foundation, administered by the American Chemical Society (ACS-PRF 42751-AC10). Parts of this work were carried out in the Institute of Technology Characterization Facility, University of Minnesota, which receives partial support from NSF through the NNIN program.

Supporting information for this article is available on the WWW under http://dx.doi.org/10.1002/anie.200803103.

connected through windows that permit mass transport of fluid precursors but limit transport of solid products after a critical size is reached. During a HT synthesis, zeolite seeds may nucleate either heterogeneously on the surface of the reactor walls or homogeneously in the void space away from the reactor walls. As shown below, nucleation can be controlled by the charge of polyelectrolytes on the reactor walls, which affects the final product morphology. The surface of 3DOM C is nearly neutral after synthesis. After oxidation in nitric acid and neutralization, carboxylate and other oxygen-containing groups are introduced on the carbon surface, providing it with a negative charge. The charge can be altered by depositing multilayers of polyelectrolytes on the surface using layer-by-layer deposition methods.[10]

TPA-silicalite-1 (hereafter referred to as silicalite) is a siliceous zeolite with the structure of ZSM-5 (Figure 1) and is prepared with tetrapropylammonium (TPA) ions as structure-directing agent. Nucleation and growth of the zeolite particles depend on precursor concentrations and reaction temperatures.[11] To allow monitoring of product growth in the nanoreactor arrays within a practical time frame, we chose a solution composition SiO_2/TPAOH/NaOH/H_2O of 10:2.4:0.87:114 (labeled "high silica concentration") with a HT reaction temperature of 80 °C. Pieces of 3DOM C with edge lengths of several millimeters and typical thicknesses near 1 mm were immersed in this reaction mixture for two days at a time, then washed with purified water, dried for sampling, and re-immersed in the HT synthesis mixture for additional two-day infiltration steps.

Figure 2 shows the growth progression for silicalite within 3DOM C under different conditions. For 3DOM C containing a negatively charged polyelectrolyte as the top surface layer, we would expect silicalite particles with an intrinsic negative surface potential[12] to be repelled by this surface, causing nucleation to occur primarily in the void space away from the wall. Even though this type of nucleation is not directly apparent from the SEM image obtained after sample drying (Figure 2a), comparison of product morphologies formed with outermost anionic or cationic polyelectrolyte layers (see below) provides evidence that nucleation and growth indeed started away from the surface. After one infiltration/HT reaction (IHT) for two days, most cages contain a small number of isolated seeds (see also TEM image, Figure S2 in the Supporting Information). After a second IHT cycle, the number of particles observed in each cage increases, as does their average size (Figure 2b). The surface of each sphere is corrugated, and features of separate particles are visible. This carbon/silica composite produces an unambiguous XRD pattern for silicalite (Figure S1 in the Supporting Information), and lattice fringes from the zeolite structure are visible by TEM (Figure S3 in the Supporting Information). Additional IHT cycles result in more filling of the void space

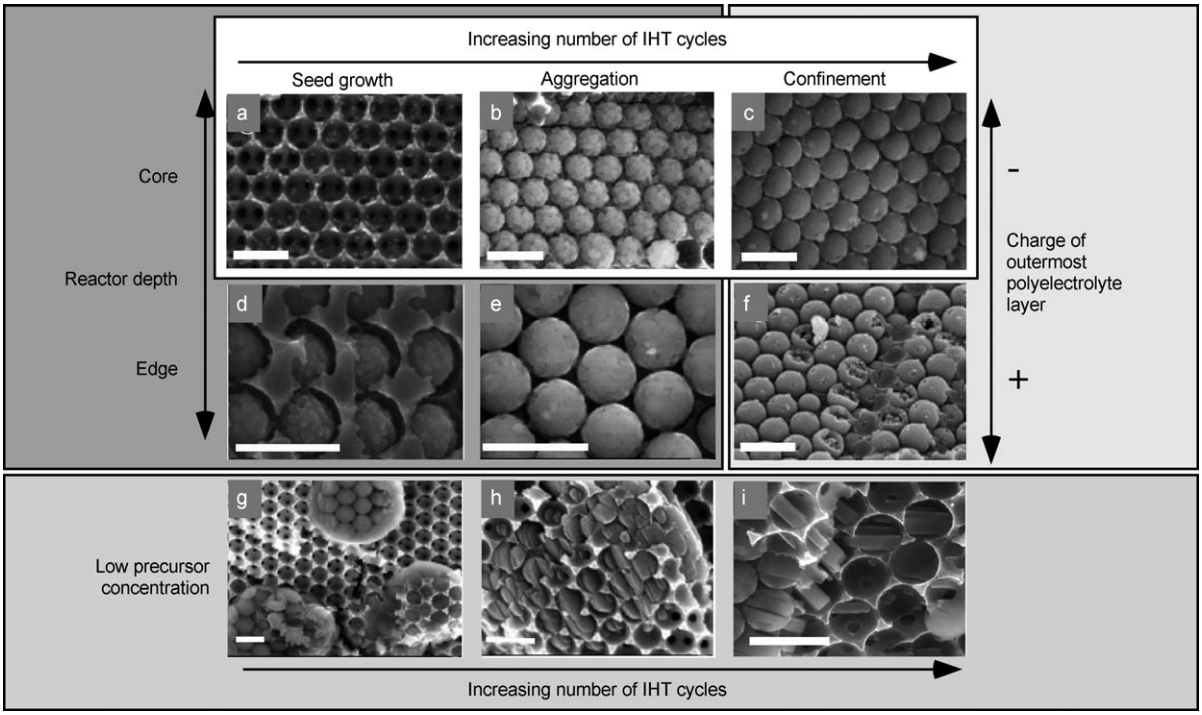

Figure 2. SEM images illustrating the different morphologies of silicalite products obtained after HT syntheses in 3DOM nanoreactors for varying processing conditions. The effect of repeated IHT cycles is shown for one, two, and four cycles (a, b, c). The images show core cross sections of 3DOM C monoliths with an outermost anionic polyelectrolyte layer for HT reactions with a high silica concentration. To illustrate the difference in product morphology between core and edge regions of the 3DOM C monolith, corresponding edge cross sections are shown for one (d) and two (e) IHT cycles. The effect of the charge of the outermost polyelectrolyte layer on particle growth is also shown (c, f). Dense spheres were produced in 3DOM C reactors with an anionic outermost polyelectrolyte (c). Hollow geode structures of silicalite particles were formed after multiple IHTs when a cationic outermost polyelectrolyte was used (f). The effect of reducing the silica precursor concentration ("low silica concentration") is shown in the SEM images after five IHT cycles (g), after seven cycles (h), and after twelve cycles (i) for silicalite prepared in 3DOM C with an anionic outermost polyelectrolyte layer. Scale bars: 500 nm.

between particles in each cage. After four or five IHT cycles, sphere sizes are limited by confinement in the macropores, and sphere surfaces are relatively smooth (Figure 2c and Figures S4 and S5 in the Supporting Information). The silicalite product is monodisperse, and nearly all macropores are filled with spheres.

In a 3DOM reactor, the morphology of the HT reaction product is, to some extent, diffusion-controlled. A concentration gradient across the monolith results in variation of the product morphology along the cross section, in particular during early IHT cycles (Figure S6 in the Supporting Information). A comparison of SEM images obtained from cross sections of the monolithic composite near the edge and in the core reveals that after a single infiltration, spherical aggregates begin to form near the edge of the sample (Figure 2d), but much of the interior contains scattered seeds (Figure 2a). After the second IHT, interparticle space is filled more for near-edge particles (Figure 2e) than in centrally located macropores (Figure 2b). The observation of smoother surfaces after subsequent cycles indicates that internal pores remain accessible to nutrients for several more IHT steps. On the basis of these relationships between sample position, reagent concentration, and product morphology, it is possible to apply combinatorial approaches to study HT growth in the 3DOM nanoreactor arrays, at least during the first few IHT cycles.

Because the reactor surface/volume ratio is high in 3DOM reactors, nucleation, growth, and morphology of the HT products depend on interfacial interactions. When the outermost polyelectrolyte layer on the reactor surface is changed from anionic to cationic, silicalite particles with negative surface charge are attracted to the wall, and crystal growth on the wall is favored. After one IHT using a 3DOM C monolith with an outermost positive polyelectrolyte layer, an SEM image (not shown) reveals a small number of isolated seeds in each cage, similar to the corresponding case for the negatively charged surface. However, after several additional IHT cycles, more material coats the carbon surface to produce spherical structures with shapes dictated by the reactor walls. An SEM image of a cross section shows several cracked spheres that are hollow and resemble geodes with shells (ca. 70 nm thick) exhibiting smooth external surfaces and textured internal surfaces (Figure 2f). Product growth therefore must have occurred mainly starting from the reactor walls into the void space, with seeds initially attached to the walls, in contrast with the situation for negatively charged reactor walls, where product grew from within the void space outwards to the walls. As windows between pores closed up, no additional nutrients could enter the system.

By reducing the silica concentration in the precursor, using a composition SiO_2/TPAOH/H_2O of 20:9:9500 ("low silica concentration"), it was possible to decrease the number of silicalite seeds within each cage and produce crystal shapes that were influenced both by the atomic crystal structure of the zeolite and by confinement effects. For this solution, reaction times for each infiltration step needed to be doubled to observe significant changes. Nucleation was delayed, but after approximately five IHT cycles, patches of spherical silicalite particles were observed (Figure 2g). After additional cycles, silicalite particles adopted morphologies of the zeolite rather than those of the reactor and spread across several adjacent macropores (Figure 2h). In some areas, needle-shaped crystals extend through windows in several adjacent macropores, their cross sections being limited by the window dimensions (Figure 2i). These results emphasize that HT product morphologies can depend on precursor concentrations, even in the confinement of a mold for nanocasting.[13] At low concentrations, product formation occurs largely by seed growth, during which a few seeds crystallize further along the predominant growth directions. When the growth direction is interrupted by a reactor wall, growth stops in this direction but can continue in other directions, as long as nutrients are available. If the growth direction is in line with a window, the crystal can grow further into another cage, but the window constriction limits crystal growth in the plane parallel to the window. In contrast, at higher precursor concentrations, more seeds are formed in each infiltration step, limiting growth of individual particles and resulting in particle agglomerates that take on the shape of the nanoreactor cages.

Upon calcination of the carbon reactors in air, monolithic, opalescent-white pieces of silicalite were obtained, which consisted of close-packed, monodisperse spheres (Figure 3). The opaline structure provides pathways for diffusion in interstitial spaces between silicalite spheres, creating a hierarchical pore structure with micropores within each silicalite particle, textural mesoporosity within each spherical agglomerate, and macroporosity at the level of the interstitial spaces. The 3D sphere array could also be converted into 2D layers. Through grinding and sonication of the zeolitic opal, the spheres were dispersed in solvents to form discrete particles, diads, triads, and some larger particle arrays. Reassembly on a planar silicon surface into polycrystalline close-packed layers was possible (Figure 3). Such monolayers of uniform zeolite particles provide a starting point for manufacturing randomly oriented molecular-sieve films by

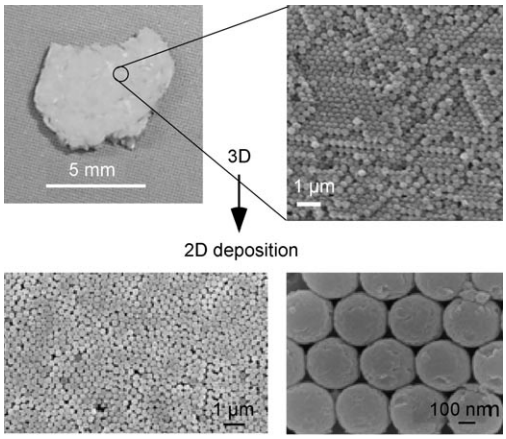

Figure 3. Photograph (top left) and SEM image (top right) of the calcined product consisting of a 3D array of close-packed silicalite spheres. Bottom: SEM images at different magnifications of a layer of spheres assembled on a flat silicon substrate after dispersion of the spheres in ethanol.

seeded growth.[14] The concepts described herein are, to some extent, scalable to reactor arrays with smaller pore sizes to form smaller spheres with similar morphologies (Figure S7 in the Supporting Information).

This study has illustrated that the morphologies of HT reaction products formed in nanocasting processes are functions not only of the shape of the mold but also of interfacial interactions, reagent transport through parallel reactor arrays, and precursor concentrations. 3DOM C monoliths proved to be particularly useful reactor arrays owing to their ease of synthesis, chemical stability, mechanical strength, interconnected pore architecture, and ability to be removed from the product by calcination. Concentration gradients through the monolith permit simultaneous observation of multiple growth stages (a type of combinatorial synthesis) during early growth stages. Eventually, most cages can be filled with product, giving an overall high yield. When HT growth occurs homogeneously and seeds are detached from the reactor walls through repulsive electrostatic interactions, solid spherical agglomerates of zeolite particles are formed, whose corrugated walls can be smoothed out by filling interparticle spaces with more nutrients. 3D arrays of discrete, monodisperse zeolite spheres are produced after calcination. Uniform hollow spheres can be recovered with heterogeneous growth from seeds that are electrostatically attached to the reactor walls. More extended needle-like structures are formed from dilute precursor solutions. The ability to control morphologies of HT products by reactor engineering on the nanometer scale has important ramifications for applications in which shape, size, and uniformity of nanoparticles influence their physical and chemical properties, or when nanoparticles need to be organized in specific ways. For example, the silicalite opal pieces (Figure 3) will provide accurate and tunable control of reaction–diffusion coupling that may improve activity and selectivity for certain reactions. On the other hand, the geodes in Figure 2 f can, in principle, be isolated as single hollow spheres with intact zeolite membrane walls and used for encapsulation, storage, and controlled-release applications. The 3DOM reactor approach also paves the way for further mechanistic studies of HT growth processes by allowing exchange of nutrients between individual reactors while restricting exchange of solid products above a minimum size determined by the reactor windows.[11] In ongoing work, we are probing the limits of 3DOM reactor engineering for even smaller pore and product dimensions and other product compositions.

Received: June 27, 2008
Revised: July 25, 2008
Published online: September 16, 2008

Keywords: colloids · hydrothermal synthesis · interfaces · template synthesis · zeolites

[1] a) G. S. Attard, J. C. Glyde, C. G. Goltner, *Nature* **1995**, *378*, 366; b) S. Polarz, M. Antonietti, *Chem. Commun.* **2002**, 2593; c) A.-H. Lu, F. Schüth, *C. R. Chim.* **2005**, *8*, 609; d) H. Yang, D. Zhao, *J. Mater. Chem.* **2005**, *15*, 1217.

[2] a) S. M. Yang, N. Coombs, G. A. Ozin, *Adv. Mater.* **2000**, *12*, 1940; b) P. Jiang, J. F. Bertone, V. L. Colvin, *Science* **2001**, *291*, 453; c) H. Míguez, N. Tétreault, S. M. Yang, V. Kitaev, G. A. Ozin, *Adv. Mater.* **2003**, *15*, 597.

[3] G. A. Ozin, *Adv. Mater.* **1992**, *4*, 612.

[4] a) M. Antonietti, E. Wenz, L. Bronstein, M. Seregina, *Adv. Mater.* **1995**, *7*, 1000; b) A. Roescher, M. Moller, *Polym. Mater. Sci. Eng.* **1995**, *72*, 283; c) K. Landfester, *Adv. Mater.* **2001**, *13*, 765; d) J. Zhang, S. Xu, E. Kumacheva, *J. Am. Chem. Soc.* **2004**, *126*, 7908.

[5] I. Schmidt, C. Madsen, C. J. H. Jacobsen, *Inorg. Chem.* **2000**, *39*, 2279.

[6] S.-S. Kim, J. Shah, T. J. Pinnavaia, *Chem. Mater.* **2003**, *15*, 1664.

[7] a) C. J. H. Jacobsen, C. Madsen, J. Houzvicka, I. Schmidt, A. Carlsson, *J. Am. Chem. Soc.* **2000**, *122*, 7116; b) A. H. Janssen, I. Schmidt, C. J. H. Jacobsen, A. J. Koster, K. P. de Jong, *Microporous Mesoporous Mater.* **2003**, *65*, 59; c) Y. Tao, H. Kanoh, K. Kaneko, *J. Am. Chem. Soc.* **2003**, *125*, 6044; d) Z. Yang, Y. Xia, R. Mokaya, *Adv. Mater.* **2004**, *16*, 727; e) J. Wang, A. Vinu, M.-O. Coppens, *J. Mater. Chem.* **2007**, *17*, 4265; f) H. Li, Y. Sakamoto, Z. Liu, T. Ohsuna, O. Terasaki, M. Thommes, S. Che, *Microporous Mesoporous Mater.* **2007**, *106*, 174.

[8] a) A. A. Zakhidov, R. H. Baughman, Z. Iqbal, C. Cui, I. Khayrullin, O. Dantas, J. Marti, V. G. Ralchenko, *Science* **1998**, *282*, 897; b) M. W. Perpall, K. P. U. Perera, J. DiMaio, J. Ballato, S. H. Foulger, D. W. Smith, Jr., *Langmuir* **2003**, *19*, 7153; c) S. B. Yoon, G. S. Chai, S. K. Kang, J.-S. Yu, K. P. Gierszal, M. Jaroniec, *J. Am. Chem. Soc.* **2005**, *127*, 4188; d) J. Lee, J. Kim, T. Hyeon, *Adv. Mater.* **2006**, *18*, 2073.

[9] K. T. Lee, J. C. Lytle, N. S. Ergang, S. M. Oh, A. Stein, *Adv. Funct. Mater.* **2005**, *15*, 547.

[10] a) G. Decher, *Science* **1997**, *277*, 1232; F. Caruso, *Adv. Mater.* **2001**, *13*, 11; b) Z. Wang, N. S. Ergang, M. A. Al-Daous, A. Stein, *Chem. Mater.* **2005**, *17*, 6805.

[11] T. M. Davis, T. O. Drews, H. Ramanan, C. He, J. Dong, H. Schnablegger, M. A. Katsoulakis, E. Kokkoli, A. V. McCormick, R. L. Penn, M. Tsapatsis, *Nat. Mater.* **2006**, *5*, 400.

[12] V. Nikolakis, M. Tsapatsis, D. G. Vlachos, *Langmuir* **2003**, *19*, 4619.

[13] B. Wucher, W. Yue, A. N. Kulak, F. C. Meldrum, *Chem. Mater.* **2007**, *19*, 1111.

[14] Z. Lai, G. Bonilla, I. Diaz, J. G. Nery, K. Sujaoti, M. A. Amat, E. Kokkoli, O. Terasaki, R. W. Thompson, M. Tsapatsis, D. G. Vlachos, *Science* **2003**, *300*, 456.

